

## RESEARCH ARTICLE

# Synthesis of Magnesium Oxide Layer on the Surface of Magnesium by the Anodizing Process for Biodegradable Implants

Mohammed A. Jawad<sup>1</sup>, Abed J. Kadhim<sup>2</sup>, Mustafa M. Kadhim<sup>3</sup>, Ayad F. Alkaim<sup>4</sup>

<sup>1,2</sup>*Al-Nisour University College, Baghdad, Iraq*

<sup>3</sup>*Department of Dentistry, Kut University College, Kut, Wasit, Iraq*

<sup>4</sup>*College of Science for Women, University of Babylon, Hillah, Iraq*

*Received: 23rd April, 2021; Revised: 07th July, 2021; Accepted: 19th August, 2021; Available Online: 25th September, 2021*

## ABSTRACT

Magnesium (Mg) as a biodegradable implant has revolutionized medical field applications, particularly in bone implants and stents. The surface of magnesium alloys used in biomedical applications was treated in this work by “anodizing in 3.5 mol/L sulfuric acids” at room temperature with (8.5V). The magnesium oxide (MgO) layer thus formed was characterized with by scanning electron microscopy (SEM), X-ray diffraction (XRD) and atomic forced spectroscopy (AFM).

The morphology and topographic structures for the MgO layer formed on the Mg surface by SEM and AFM techniques show the oxide layer is porous in nature; this porous oxide layer will enable the bone tissue to infiltrate them, healing the bone tissue pretty earlier.

The corrosion behavior of the Mg alloy was examined by means of electrochemical techniques and potential polarization curves at temperatures between 298 and 328 K in saline conditions. The alloy was increased corrosion protection with increasing temperatures from 99.93 to 99.97%, indicate the MgO layer formed on the Mg surface was not affected by temperature. The pre-exponential factor “kinetic parameters” and activation energy “kinetic parameters” were discussed calculated. Thermodynamic activation values S and H were also estimated.

**Keywords:** Anodizing, Biomedical, Bone implant, Corrosion, Magnesium alloy.

International Journal of Pharmaceutical Quality Assurance (2021); DOI: 10.25258/ijpqa.12.3.12

**How to cite this article:** Jawad MA, Kadhim AJ, Kadhim MM, Alkaim AF. Synthesis of Magnesium Oxide Layer on the Surface of Magnesium by the Anodizing Process for Biodegradable Implants. International Journal of Pharmaceutical Quality Assurance. 2021;12(3):223-228.

**Source of support:** Nil.

**Conflict of interest:** None

## INTRODUCTION

Magnesium alloys are gaining popularity as structural materials, and they are being used more frequently. The biodegradability of Mg has attracted the attention of researchers to avoid secondary surgery to remove the implant materials after the healing process. Mg's various advantages make it suitable for medical application such as density, good mechanical properties, and biodegradation.<sup>1,2</sup> Mg<sup>2+</sup> is the fourth most important ion in the human body, with the majority of it being kept in bones. It is a component in many enzymes and a critical component of the ribosomal apparatus, which converts the genetic data stored by mRNA into polypeptide structures.<sup>3,4</sup>

Mg and its alloy, on the other hand, have a low resistance to corrosion due to their strong surface chemistry,<sup>5</sup> which has limited their use within the aforementioned applications, particularly in harsh settings.<sup>6</sup> So because corrosion rate is supposed to be low in the initial stage due to the changed surface layer, surface treatment of Mg alloys is of special relevance for possible implantation.<sup>7</sup>

Many surface treatment methods for the preservation of mag or magnesium alloys have been created over the last few years, including electrolytic plating, conversion coatings, anodizing, laser surface alloying, and biological surface coating.<sup>8</sup> Anodizing therapy is among the most effective procedures for magnesium alloys among these techniques.<sup>9,10</sup> An oxide layer is generated at the top of the magnesium or magnesium alloy utilizing a high voltage electricity source in an acidic electrolyte in this anodizing process.

Anodizing is an electrolytic process for producing a thick, stable oxide film on metals and alloys. These films may be used to improve paint adhesion to the metal, as a key for dyeing or as a passivation treatment.

This research looks into using an anodizing method in an acidic “H<sub>2</sub>SO<sub>4</sub>” solution to create a MgO layer on magnesium alloys for surface treatment in orthopedic applications. Potentiodynamic polarization tests in a corrosive 3.5 wt. percent NaCl solution was used to evaluate the anti-corrosion capabilities of the oxide layer formed on magnesium alloy.

\*Author for Correspondence: mohammed.a.medical.lab@nuc.edu.iq

The form and content of the MgO layer were next investigated using scanning electron microscopy (SEM), atomic force microscopy (AFM), and X-ray diffraction techniques (XRD).

## EXPERIMENTAL PART

### Magnesium Alloy Preparation

Magnesium alloys with a surface area of 1.51.5 cm<sup>2</sup> were purchased as 0.5 mm thick sheets via Amazon. The magnesium board was refined using mesh emery sheets of 600, 1200, and 2000, and the alloy samples were cleansed before the air was evaporated with distilled water, ethanol, and finally acetone.

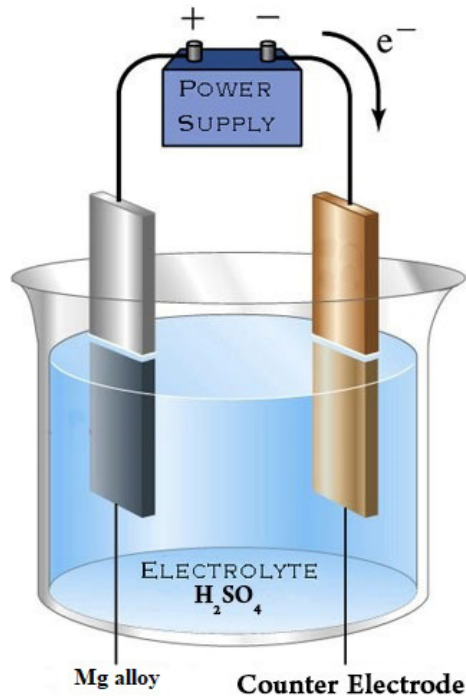


Figure 1: Anodizing magnesium cell<sup>11</sup>

The specimens were deoxidized with 10% NaOH and then de-smutted with 50% nitric acid before anodization, followed by a dual rinse by distilled water and acetone.<sup>11</sup>

### Corrosive Media Preparation (saline solution)

In order to maintain a white solution of the saline medium, sodium chloride (35 gram) was dissolved in 1-L distilled water. Choose 3.5 percent of NaCl in this trial to avoid ohms-related difficulties.

### Anodizing Process of Magnesium

A two-electrode cell was used for the dip - coating procedures, with a huge titanium sheet serving as the counter electrode. The electrolyte was 3.5 mol/L  $H_2SO_4$  solution, and the spacing electrodes was 3-4 cm. anodizing at a voltage of 8.5 volts and a period of 15 minutes at room temperature. The magnesium was washed thoroughly and dried with an air dryer after the anodizing procedure. The anodizing cell is depicted in Figure 1.

### Characterization and Test

XRD, AFM, and SEM were used to measure and characterize the surface morphologies of the magnesium oxide layer generated by anodizing. WENKING M Lab was used to measure Galvanostatic polarization (Germany). Before and after anodizing treatment, polarization curves for magnesium alloy were produced. The cathodic and anodic zones were implicated in the polarization curve. The extended method can be employed for the purposes of calculating corrosion current ( $i_{corr}$ ) and corrosion potential ( $E_{corr}$ ) by examining each polarizing area in greater detail.<sup>12</sup>

## RESULT AND DISCUSSION

### Structure and Morphology of Surfaces

The surface Morphology of the oxide layer plays an significant part in increasing “the corrosion” protection efficiency (PE%). More uniform grains may lead to more

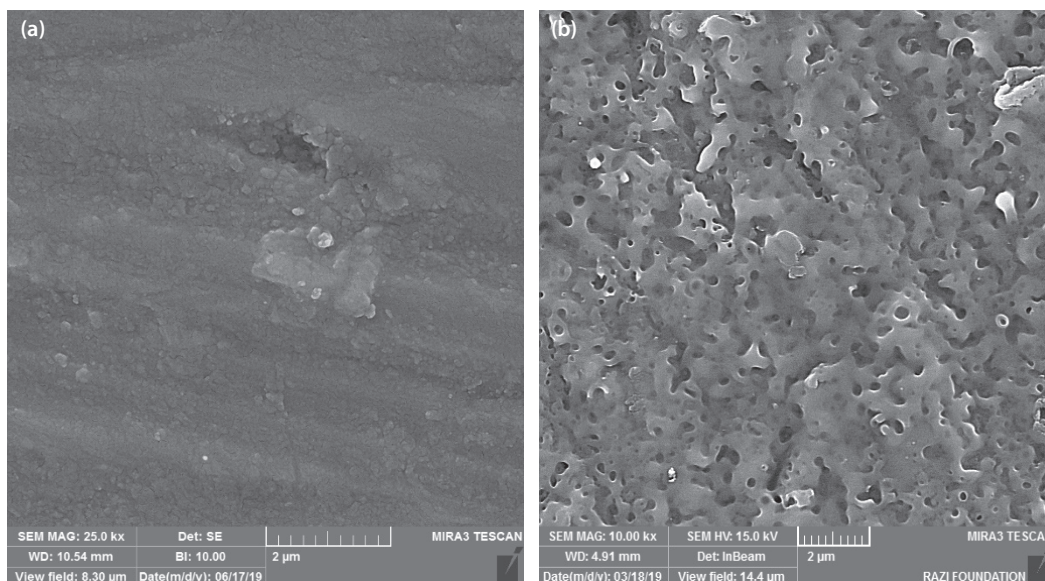


Figure 2: SEM images for Mg (a) before anodizing and (b) after anodizing.

corrosion resistance results. SEM image showed more clear shape additionally for the clustering and particles load on metals surfaces. 2D, 3D views of AFM images for coated layers and statistical determination were used to determine particle size distribution. SEM and AFM techniques showed the morphology and topographic structures of the magnesium “oxide layer” formed on “Mg alloys” by anodizing (Figure 2). The holes were properly separated and spread homogeneously throughout the surface with a medium diameter (300 nm). The porous “of oxide layer on Mg” surface will enable the bone tissue to infiltrate them, healing the bone tissue pretty earlier.<sup>13</sup>

Figure 3 shows similar pore formation is observed with average grains nearly equal to (39.7 nm).

X-ray scattering (XRD) investigation to determine variations in oxide produced in the acid electrolyte composition has been undertaken (Figure 4). The pattern of diffraction clearly demonstrates that the films comprise of MgO and

magnesium impurities trace proportions. The creation of a crystalline MgO state is illustrated by simultaneous stage training at anodic film/electrolyte and magnesium substratum/film interface, by the movement from the substratum to the anodic coating/electrolyte Interface of Mg+2 ions outwards.

Figure 1 shows the “X-ray diffraction spectra” of Mg before and after anodizing in acidic solution.<sup>4</sup> Figure (4a) shows the peaks at 2 degrees (35.5, 38.8, 40.5, 53.3, 63.3, 71, and 76.6), which are in good agreement with the distinctive peaks of magnesium (100, 002, 101, 102, 110, 103, and 112) correspondingly. Small peaks were reflected at 2 (25.4, 36.3, 71.5, and 77.5) degrees in figure (4b), and these peaks referred to the crystal structure of the current magnesium oxide generated by anodizing. And the titanium’s distinctive peaks moved to a lower 2theta degree.

The sample crystallite dimension was determined with the approximation of Debye–Scherrer from complete width to half the peaks (FWHM) (Eq. 1).<sup>14</sup>

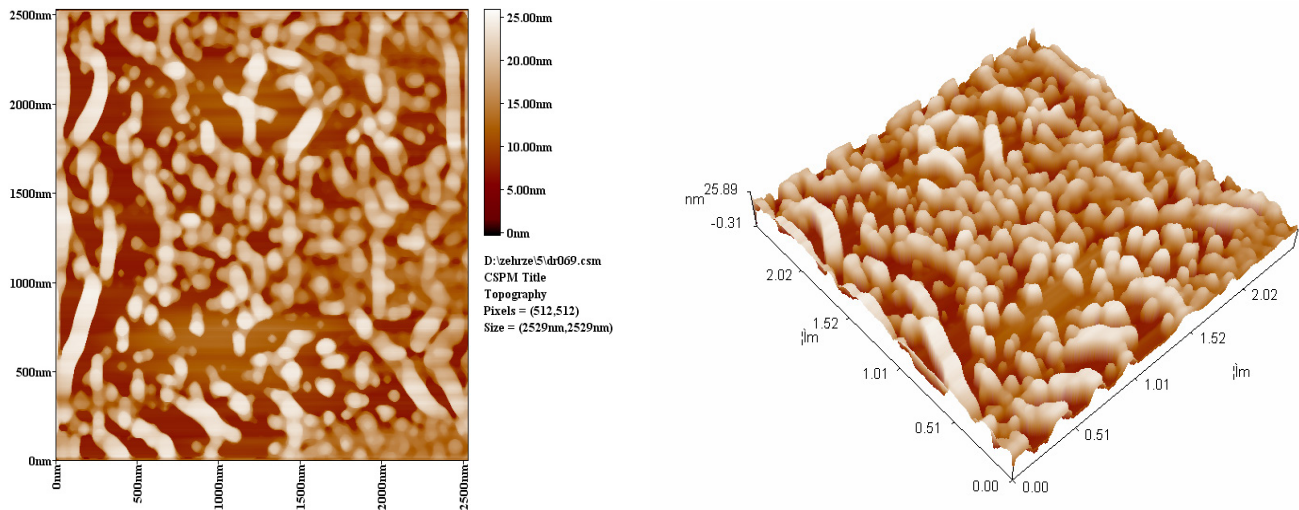


Figure 3: 2D and 3D views of AFM image for Mg after anodizing by sulfuric acid.

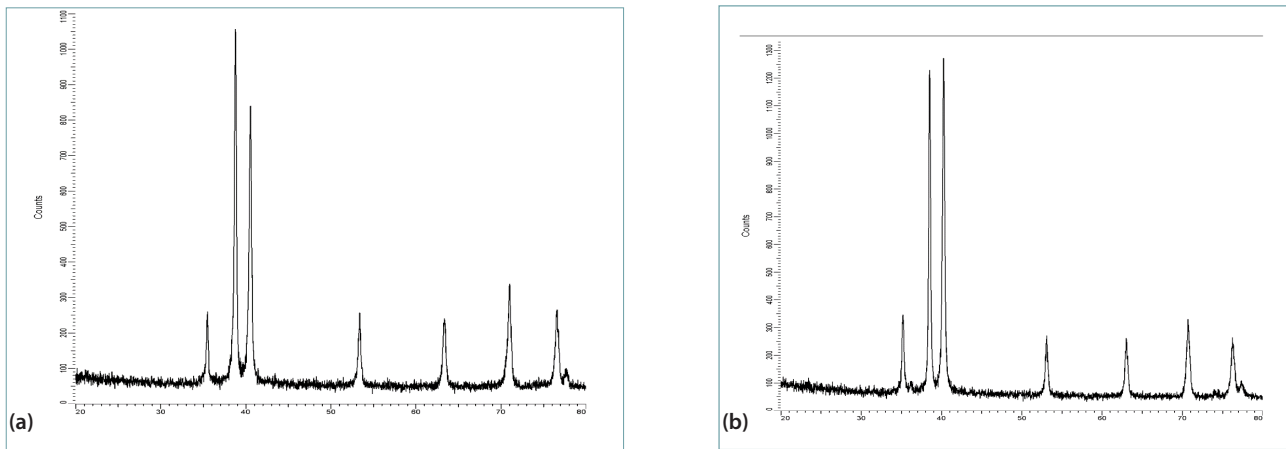


Figure 4: XRD patterns for Mg alloy (a) before anodizing, (b) after anodizing.

$$d = \frac{k\lambda}{\beta \cos\theta} \quad (1)$$

Where d is the size of the crystallite, k is the wavelength of CuKa ( $k = 1.542\text{\AA}$ ),  $\beta$  is the FWHM (radians),  $\theta$  is the diffraction angle and k is the broadening constant ( $k = 0.9$ ). The crystallite size has been detected for Mg and was the average size equal to 227.5 nm.

**Corrosion Test**

The figure shows the Tafel graphs for corrosion tests on Mg alloys submerged in artificial saliva before and after anodizing by acidic solution at various temperatures (5). Percentage protection efficiency from Tafel polarization (%PE) was listed in Table 1. These values were calculated using the following equation:<sup>15</sup>

$$\%PE = \frac{i_{corr}^o - i_{corr}}{i_{corr}^o} \times 100 \quad (2)$$

Where  $i_{corr}^o$  and  $i_{corr}$  are the corrosion rate for Mg alloys before and after anodizing process, respectively.

Table 1. shows that the values of  $\beta_a$  and  $\beta_c$  are not much different. This indicated that both anodic and cathodic reactions were controlled by the MgO on the surface of Mg alloy.

The values of  $I_{corr}$  decreased by a layer of oxide on a metal surface that prevented metal interaction with corrosive media.<sup>16</sup>

The protective effectiveness has a direct relationship to the temperature as shown in Figure 5. This is chiefly due to a thin oxide layer preventing the formation of a saline environment on the metal surface. With the formation of MgO layer on the surface of the metal, the corrosion potential was shifted to active potential but did not change significantly with the temperature.<sup>17</sup>

Based on the equation Stern–Geary, small polarization near the corrosion potential is performed to determine corrosion resistance:<sup>17</sup>

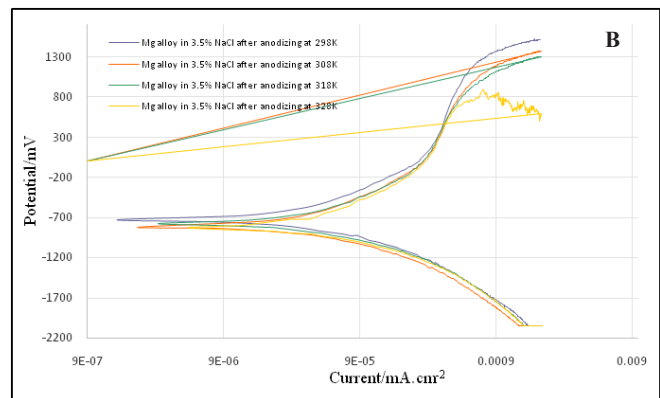
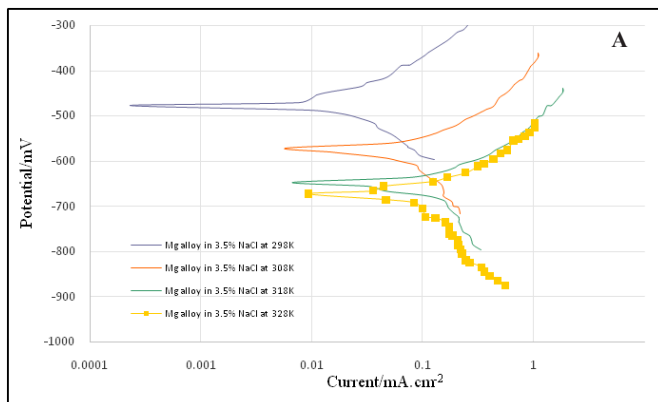
$$R_p = \frac{b_a b_c}{2.303(b_a + b_c)} \cdot \frac{1}{i_{corr}} \quad (3)$$

where  $R_p$  is the polarization resistance of the system, the corrosion current density  $i_{corr}$ ,  $b_a$ , and  $b_c$  are the anodic and cathodic Tafel coefficients, respectively.

Polarization resistance for debate is very useful in recognizing and restarting the action of corrosion problems and demands to measure the complete polarization curves.<sup>18</sup> For anodization, Mg alloy polarization resistance (RP) values were greater than  $R_p$  for Mg alloy before anodization and have increased from (298 to 328) K at increased temperature.

**Table 1:** Corrosion kinetic parameters for Mg alloys in saline at different temperatures.

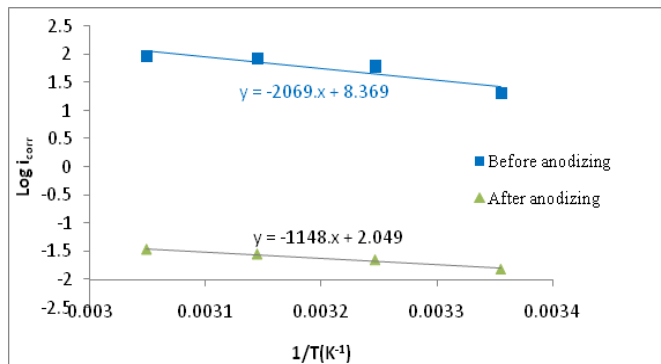
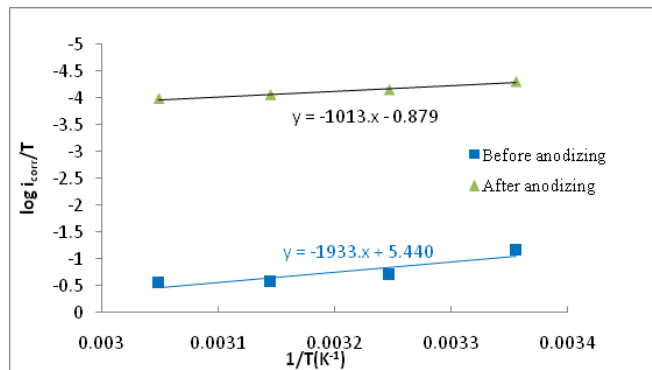
| “Temp./K”                 | “ $E_{corr}/mV$ ” | “ $I_{corr}/\mu A.cm^{-2}$ ” | “ $\beta_a/mV.dec^{-1}$ ” | “ $\beta_c/mV.dec^{-1}$ ” | “%PE” | “ $R_p/k\Omega.cm^2$ ” |            |
|---------------------------|-------------------|------------------------------|---------------------------|---------------------------|-------|------------------------|------------|
| Mg alloy before anodizing | 298               | 478.5                        | 20.64                     | 159.6                     | 161.5 | -                      | 1688.735   |
|                           | 308               | 571.7                        | 61.16                     | 106.5                     | 231.2 | -                      | 517.660    |
|                           | 318               | 647.8                        | 85.33                     | 94.4                      | 91.2  | -                      | 236.044    |
|                           | 328               | 672.5                        | 91.9                      | 123.3                     | 322.1 | -                      | 421.303    |
| Mg alloy after anodizing  | 298               | 744.1                        | 0.015                     | 478.6                     | 246.8 | 99.93                  | 4713625.79 |
|                           | 308               | 808.4                        | 0.022                     | 638.6                     | 386.6 | 99.96                  | 4752975.19 |
|                           | 318               | 768.7                        | 0.028                     | 631.9                     | 425.2 | 99.97                  | 3941609.26 |
|                           | 328               | 820.4                        | 0.034                     | 817.5                     | 450.8 | 99.96                  | 3710879.23 |



**Figure 5:** Mg alloy polarization plots in saline medium at 298-328 K range; a) before anodizing and b) after anodizing.

**Table 2:** Kinetic parameters of Mg alloys before and after anodizing in saline media.

| “Solution”                | “ $\Delta H^*$ ”<br>“(kJ.mol <sup>-1</sup> )” | “ $\Delta S^*$ ”<br>“(kJ.mol <sup>-1</sup> .K <sup>-1</sup> )” | “ $E_a$ ”<br>“(kJ.mol <sup>-1</sup> )” | “A”<br>“Molec.cm <sup>-2</sup> .s <sup>-1</sup> ” |
|---------------------------|---|--|--|---|
| Mg alloy before anodizing | 37.03   | -0.0934  | 39.626                                 | 1.41×10 <sup>26</sup>                             |
| Mg alloy after anodizing  | 19.40   | -0.2144  | 21.998                                 | 6.75×10 <sup>25</sup>                             |


**Figure 6:** Arrhenius plot of  $\log i_{\text{corr}}$  versus  $1/T$  for the corrosion of Mg alloy in saline solution”.

**Figure 7:** A plot of  $\log i_{\text{corr}}/T$  Vs.  $1/T$  for the corrosion of Mg alloy in saline solution”.

### Effect of Temperature and Kinetics Studies

The effect of temperature on the corrosion reaction Mg alloy before and after anodizing in saline solutions was studied at a range of 298–328K. According to Table 1, the reaction rate ( $i_{\text{corr}}$ ) was increased with temperature. This behavior can be well-understand using Arrhenius equation (Eq. 4) and transition state equation (Eq. 5):<sup>19</sup>

$$\log i_{\text{corr}} = \frac{-E_a}{2.303RT} + \log A \quad (4)$$

$$\log \frac{i_{\text{corr}}}{T} = \log \frac{R}{Nh} + \frac{\Delta S^*}{2.303R} - \frac{\Delta H^*}{2.303RT} \quad (5)$$

Where “ $E_a$  represents the activation energy of the corrosion process,  $R$  is the gas constant ( $R \approx 8.314 \text{ J.K}^{-1}.\text{mol}^{-1}$ ),  $A$  is the pre-exponential factor,  $h$  is the Plank’s constant ( $6.626176 \times 10^{-34} \text{ Js}$ ),  $N$  is the Avogadro’s number ( $6.022 \times 10^{23} \text{ mol}^{-1}$ ),  $\Delta S^*$  is the entropy of activation, and  $\Delta H^*$  is the enthalpy of activation”. These equations can be plotted as  $\log i_{\text{corr}}$  and  $\log i_{\text{corr}}/T$  against reciprocal of absolute temperature, respectively (Figure 6 and 7). Slopes and intercepts of these equations can be used to evaluate the kinetics parameters. Values of  $E_a$  and  $A$  were obtained from the slope ( $-E_a/2.303R$ ) and intercept ( $\log A$ ) of Eq. 4, respectively. While values of  $\Delta H^*$  and  $\Delta S^*$  were obtained from the slope ( $-\Delta H^*/2.303R$ ) and an intercept  $[(\log(R/Nh) + (\Delta S^*/2.303R))]$  of Eq. 5, respectively. The results were collected in Table 2.

After anodizing Mg alloy, the value of  $H^*$  falls, forming an oxide layer that requires less energy to dissolve, resulting in an endothermic reaction to achieve equilibrium.<sup>20</sup>

The data suggest that the energizing power dropped after acidic anodized, the number of sites of corrosion reduced on Mg alloys surface after therapy by anodizing ( $39.626 \text{ kJ.mol}^{-1}$ ) to ( $21.998 \text{ kJ.mol}^{-1}$ ) as well as the number of Arrhenius sites after therapy.

### CONCLUSION

In this is work, the treatment of Mg alloys surface by anodizing in acidic media and its structural, morphological, and compositional properties were investigated.

SEM and AFM images shows the oxide layer formed on the surface have pores that were well separated and homogeneously distributed over the whole surface, with an average diameter of around 300 nm and the porous of oxide layer on the Mg surface will enable the bone tissue to infiltrate them healing the bone tissue pretty earlier. The XRD pattern for Mg alloys before and after anodizing shows small peaks were reflected at  $2\theta$  (25.4, 36.3, 71.5, and 77.5) degrees. These peaks referred to the crystal structure of the present magnesium oxide formed by Anodizing. And the characteristic peaks of titanium slightly shifted to less  $2\theta$  degree.

Temperatures had no effect on the protective efficacy of Mg alloy after anodizing, which varied from 99.93–99.97% PE. After anodizing, the activating value of titanium corrosion reduces, indicating that the structure of the titanium surface (oxide layer shape) has changed and is now more solid.

### REFERENCES

- Emley E. Principles of magnesium technology Pergamon Press. New York, London. 1966.
- Zhang Y, Yan C, Wang F, Lou H, Cao C. Study on the environmentally friendly anodizing of AZ91D magnesium alloy. Surface and Coatings Technology. 2002 Nov 1;161(1):36-43.
- Hartwig A. Role of magnesium in genomic stability. Mutation Research/Fundamental and Molecular Mechanisms of Mutagenesis. 2001 Apr 18;475(1-2):113-21.
- Staiger MP, Pietak AM, Huadmai J, Dias G. Magnesium and its alloys as orthopedic biomaterials: a review. Biomaterials. 2006 Mar 1;27(9):1728-34.
- Makar GL, Kruger JL. Corrosion of magnesium. International materials reviews. 1993 Jan 1;38(3):138-153.

6. Almashhdani H, Alsaadie K. Corrosion Protection of Carbon Steel in seawater by alumina nanoparticles with poly (acrylic acid) as charging agent. *Moroccan Journal of Chemistry*. 2018 Apr 29;6(3):455-465.
7. Mohammed RA, AL-mammar DE. Using natural materials as corrosion inhibitors for carbon-steel on phosphoric acid medium. *Iraqi Journal of Science*. 2019 Apr 18:40-45.
8. Gray J, Luan B. Protective coatings on magnesium and its alloys—a critical review. *Journal of alloys and compounds*. 2002 Apr 18;336(1-2):88-113.
9. Shi Z, Song G, Atrens A. The corrosion performance of anodised magnesium alloys. *Corrosion Science*. 2006 Nov 1;48(11):3531-3546.
10. AlMashhadani HA, Saleh KA. Electrochemical Deposition of Hydroxyapatite Co-Substituted By Sr/Mg Coating on Ti-6Al-4V ELI Dental Alloy Post-MAO as Anti-Corrosion. *Iraqi Journal of Science*. 2020 Nov 28:2751-2761.
11. AlMashhadani HA. Corrosion Protection of Pure Titanium Implant by Electrochemical Deposition of Hydroxyapatite Post-Anodizing. In *IOP Conference Series: Materials Science and Engineering* 2019 Jul 1 (Vol. 571, No. 1, p. 012071). IOP Publishing.
12. Al-Mammar DE, Mohammed RA. Study The Antibacterial Activity And Inhibition Effect Of Reactive Red (31) Dye For The Corrosion Of Carbon Steel In Corrosive Media. *Iraqi Journal of Market Research and Consumer Protection*. 2019 Apr 25;11(1):123-130.
13. AlMashhadani HA. Surface Treatments of Some Titanium Biomedical Dental Alloys for Corrosion Protection Enhancement and Anti-Microbial Applications, University of Baghdad, College of Science, Chemistry Department. 2020.
14. Giri PK, Goswami DK, Perumal A, editors. *Advanced Nanomaterials and Nanotechnology: Proceedings of the 2nd International Conference on Advanced Nanomaterials and Nanotechnology*, Dec 8-10, 2011, Guwahati, India. Springer Science & Business Media; 2013 Mar 17.
15. AlMashhadani HA. Corrosion protection of pure titanium implant in artificial saliva by electro-polymerization of poly eugenol. *Egyptian Journal of Chemistry*. 2020 Aug 1;63(8):2-3.
16. Abbas HA, Alsaade KA, AlMashhdan HA. Study the effect of cyperus rotundus extracted as mouthwash on the corrosion of dental amalgam. In *IOP Conference Series: Materials Science and Engineering* 2019 Jul 1 (Vol. 571, No. 1, p. 012074). IOP Publishing.
17. AlMashhadani HA, Saleh KA. Electrochemical Deposition of Hydroxyapatite Co-Substituted By Sr/Mg Coating on Ti-6Al-4V ELI Dental Alloy Post-MAO as Anti-Corrosion. *Iraqi Journal of Science*. 2020 Nov 28:2751-2761.
18. AlMashhadani HA, Saleh KA. Electro-polymerization of poly Eugenol on Ti and Ti alloy dental implant treatment by micro oxidation using as Anti-corrosion and Anti-microbial. *Research Journal of Pharmacy and Technology*. 2020 Oct 1;13(10):4687-4696.
19. Al-Mashhadani HA, Alshujery MK, Khazaal FA, Salman AM, Kadhim MM, Abbas ZM, Farag SK, Hussien HF. Anti-Corrosive Substance as Green Inhibitor for Carbon Steel in Saline and Acidic Media. In *Journal of Physics: Conference Series* 2021 Mar 1 (Vol. 1818, No. 1, p. 012128). IOP Publishing.
20. Hameed RA, Ismail EA, Abu-Nawwas AH, Al-Shafey HI. Expired Voltaren drugs as corrosion inhibitor for aluminium in hydrochloric acid. *Int J Electrochem Sci*. 2015 Mar 1;10:2098-2109.